

Roles for Ephrins in Positionally Selective Synaptogenesis between Motor Neurons and Muscle Fibers

Guoping Feng,*# Michael B. Laskowski,*†#
David A. Feldheim,‡ Hongmin Wang,† Renate Lewis,*
Jonas Frisen,§ John G. Flanagan,‡
and Joshua R. Sanes*||

*Department of Anatomy
Washington University Medical School
St. Louis, Missouri 63110

†WWAMI Medical Program
University of Idaho
Moscow, Idaho 83844

‡Department of Cell Biology
Harvard Medical School
Boston, Massachusetts 02115

§Department of Cell and Molecular Biology
Medical Nobel Institute
Karolinska Institute
Stockholm S17177
Sweden

Summary

Motor axons form topographic maps on muscles: rostral motor pools innervate rostral muscles, and rostral portions of motor pools innervate rostral fibers within their targets. Here, we implicate A subfamily ephrins in this topographic mapping. First, developing muscles express all five of the *ephrin-A* genes. Second, rostrally and caudally derived motor axons differ in sensitivity to outgrowth inhibition by ephrin-A5. Third, the topographic map of motor axons on the gluteus muscle is degraded in transgenic mice that overexpress ephrin-A5 in muscles. Fourth, topographic mapping is impaired in muscles of mutant mice lacking ephrin-A2 plus ephrin-A5. Thus, ephrins mediate or modulate positionally selective synapse formation. In addition, the rostrocaudal position of at least one motor pool is altered in ephrin-A5 mutant mice, indicating that ephrins affect nerve-muscle matching by intraspinal as well as intramuscular mechanisms.

Introduction

Neurons in many parts of the nervous system form topographically ordered maps of synaptic connections on their targets. In the peripheral motor system, the map takes the form of a consistent relationship between the position of motoneurons along the rostrocaudal axis of the spinal cord and the position of the skeletal muscle fibers that the motoneurons innervate. This relationship is evident at both intermuscular and intramuscular levels: successively more caudal muscles are innervated by successively more caudal sets (pools) of motoneurons, and successively more caudally located muscle fibers within many individual muscles are innervated by successively more caudally disposed motoneurons from

that muscle's motor pool (Browne, 1950; Swett et al., 1970; Laskowski and Sanes, 1987).

Although proximity of the synaptic partners during development no doubt contributes to this positional matching, there is compelling evidence that mapping also depends on recognition of intramuscular cues by motor axons. First, muscles transplanted from distinct axial levels to a common site are selectively reinnervated by axons corresponding to their position of origin (Wigston and Sanes, 1982, 1985). Second, even when axons from many segmental levels reach a muscle through a single peripheral nerve, they form topographic maps within the muscle (Laskowski and Sanes, 1987). Third, some such maps are sharpened by an intramuscular process of synapse elimination after connections have formed (Brown and Booth, 1983; Bennett and Lavidis, 1984; Bennett and Ho, 1988). Finally, intramuscular maps are partially restored during reinnervation following axotomy, even though all regenerating axons have equal and simultaneous access to the muscle (Hardman and Brown, 1987; Laskowski and Sanes, 1988; DeSantis et al., 1992; Laskowski et al., 1998). Together, these results suggest that motor axons and some intramuscular structures bear complementary molecular labels that vary with rostrocaudal position and that bias synapse formation in favor of positionally matched partners. To date, however, none has been described.

Here, we present evidence that ephrins of the A subfamily mediate or modulate positionally selective synaptogenesis between motor axons and muscle fibers. The ephrins are a large family of membrane-associated ligands for the even larger Eph family of receptor tyrosine kinases (reviewed by Flanagan and Vanderhaeghen, 1998; Zhou, 1998). The ephrins are divisible into two groups: five ephrins-A, which are tethered to the membrane by a glycosylphosphatidylinositol linkage, and three ephrins-B, which are transmembrane proteins. Similarly, the Eph kinases form two subfamilies, A (eight members) and B (six members), based on sequence similarity. Ephrins-A bind selectively to EphA kinases as do ephrins-B to EphB kinases, but interactions are promiscuous within subfamilies—most ephrins-A bind most EphA kinases, and so on (Brambilla et al., 1996; Gale et al., 1996).

During the past few years, evidence has accumulated that activation of EphA kinases on the axons of retinal ganglion cells by ephrins-A on cells of the optic tectum (superior colliculus) plays a critical role in mapping the rostrocaudal axis of the retina onto the corresponding axis of the tectum (Cheng et al., 1995; Drescher et al., 1995; Nakamoto et al., 1996; Monschau et al., 1997; Ciossek et al., 1998; Frisen et al., 1998; reviewed by Flanagan and Vanderhaeghen, 1998; Holder and Klein, 1999; O'Leary and Wilkinson, 1999). The similarities between topographic maps in the motor and visual systems suggested that similar molecular mechanisms might underlie them (Sanes, 1993). Several recent observations are consistent with this possibility. First, ephrin-A5 is expressed in developing muscles; indeed, we independently isolated ephrin-A5 by subtractive hybrid-

|| To whom correspondence should be addressed (e-mail: sanesj@thalamus.wustl.edu).

These authors contributed equally to this work.

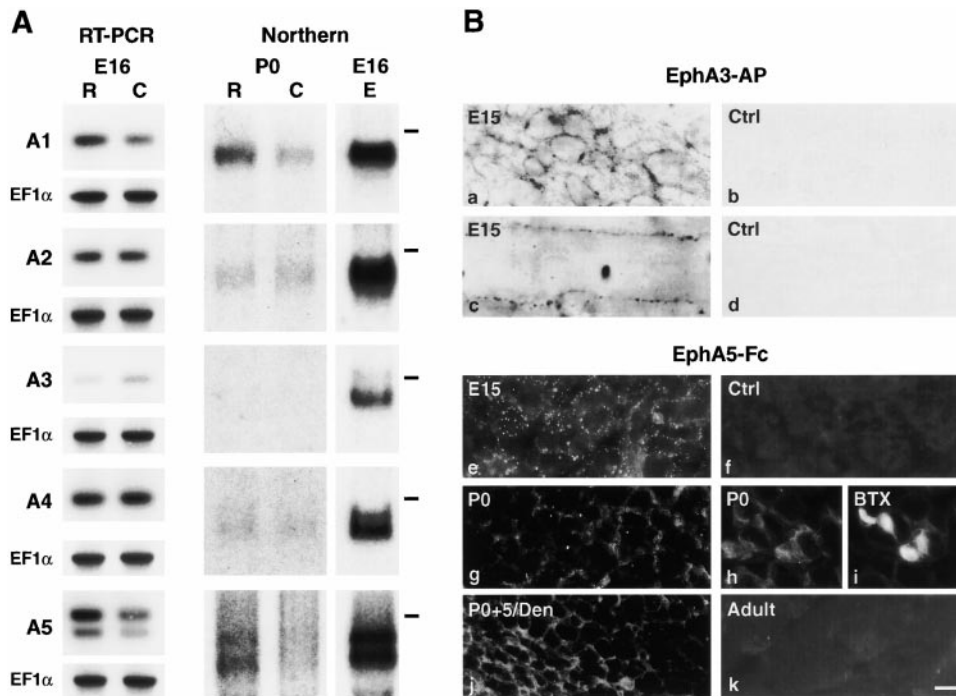


Figure 1. Expression of Ephrins-A in Muscle

(A) Ephrin-A1-A5 RNAs in shoulder and forelimb (rostral, R) and thigh and hindlimb (caudal, C) muscles from E16 embryos (left column) and neonatal mice (right columns). RNAs were detected by quantitative RT-PCR in embryonic muscle and by Northern blotting in neonatal muscle. At both ages, ephrin-A1, -A2, -A4, and -A5 RNAs were readily detected, with ephrin-A1 and ephrin-A5 RNAs being 2- to 4-fold more abundant in rostral than in caudal muscle. In the experiment shown here, the ratio of product (R/C) was 2.3, 1.0, 0.5, 1.0, and 2.0 for A1-A5, respectively. EF-1 α primers were used in RT-PCR to ensure equal input (left), and EF-1 α cDNA was used to reprobe Northern blots to ensure equal loading (data not shown). Northern blotting of whole E16 embryos (column marked "E") showed that RNAs in muscle were the same size as those in embryos. Markers indicate the position of the 2.4 kb standard for ephrins-A1-A4 and 9.5 kb standard for ephrin-A5.

(B) Sections of muscle stained with EphA3-AP or EphA5-Fc fusion proteins, which bind to ephrins-A but not to ephrins-B. Ephrins-A were present on myotube surfaces at E15 (Ba and Be); levels declined perinatally (Bg), both synaptically and extrasynaptically (Bh and Bi), and no expression was detectable in adults (Bk). Longitudinal section of a muscle that was stained live prior to sectioning showed that ephrins were extracellular. A single myotube is shown at high magnification (Bc). Control proteins (Fc, AP, or EphB-Fc) did not stain (Bb, Bd, and Bf; data not shown). (Bi) shows the same field as (Bh), counterstained with rhodamine- α -bungarotoxin (BTX) to mark synaptic sites. Denervation of neonatal (Bj) and adult (data not shown) muscle led to increased levels of myotube-associated ephrins.

Scale bar in (Bk), 20 μ m (Ba, Bb, and Be-Bk) and 8 μ m (Bc and Bd).

ization as a gene expressed at higher levels in rostral than in caudal muscle (Donoghue et al., 1996). Second, at least three Eph kinases, EphA3-EphA5, are expressed by subsets of motoneurons (Ohta et al., 1996; Kilpatrick et al., 1996; Olivieri and Miescher, 1999). Third, axons of motoneurons, like those of retinal ganglion cells, are sensitive to ephrins (Donoghue et al., 1996; Ohta et al., 1997; Wang and Anderson, 1997). Finally, motor axons respond differentially to membranes from rostrally and caudally derived myotubes (Wang et al., 1999) in assays similar to those used to detect effects of tectal ephrins on retinal axons (Walter et al., 1987a; Drescher et al., 1995; Nakamoto et al., 1996). Based on these parallels, we hypothesized that muscle-derived ephrins mediate or modulate positionally selective synapse formation, and we designed experiments to test this hypothesis.

Results

Developmental Regulation of Ephrins-A in Muscle

We previously showed that ephrin-A5 is expressed in skeletal muscles (Donoghue et al., 1996). To begin the

present study, we asked whether other ephrins of the A subfamily are also present in muscles. RNA from rostral (shoulder and forelimb) or caudal (thigh and hindlimb) muscles of embryonic day 16 (E16) mice was assayed by quantitative RT-PCR (see Experimental Procedures) using primers specific for ephrins-A1-A5. Ephrins-A1, -A2, -A4, and -A5 were readily detectable in both rostral and caudal samples, and ephrin-A3 was present at low levels (Figure 1A, left). Ephrin-A1 and ephrin-A5 RNAs were 2- to 3-fold more abundant in rostral than in caudal muscle; ephrins-A2 and -A4 were present at similar levels in rostral and caudal muscles; ephrin-A3 appeared to be more abundant in caudal than in rostral muscle in some experiments. To confirm the difference between rostral and caudal muscles by a second method, we used Northern blotting. Neonates were used for this experiment, due to the difficulty of obtaining sufficient RNA from small subsets of embryonic muscles. Again, ephrin-A1 and ephrin-A5 RNAs were more abundant in rostral than in caudal muscle, ephrin-A2 and ephrin-A4 RNAs were equally abundant in both samples, and ephrin-A3 RNA was barely detectable (Figure 1A, right).

In all cases, ephrin RNAs were identical in size to those detected in whole embryos.

Muscles contain numerous cell types, including myoblasts, myotubes, fibroblasts, vascular cells, glial cells, and axons. To determine the cellular source of intramuscular ephrins, we stained sections with fusion proteins in which the ectodomain of an EphA kinase was fused either to the Fc fragment of a human immunoglobulin (Ig) protein (EphA5-Fc) or to alkaline phosphatase (EphA3-AP). Such fusion proteins have been shown to recognize all ephrins of the A subfamily but not those of the B subfamily (Gale et al., 1996). Ephrins-A were present in a punctate pattern on the surface of and between myotubes (Figures 1Ba and 1Be). In some experiments, live muscles were incubated with the fusion protein, then fixed and sectioned, to show that ephrins are extracellular and therefore potentially accessible to ingrowing axons (Figures 1Bc and 1Bd). Ephrins were present at lower levels on neonatal myotubes and were undetectable in adult muscle (Figures 1Bg and 1Bk). This developmental decrease in protein level mirrors that documented previously at the RNA level for ephrin-A5 (Donoghue et al., 1996). Similar results were obtained with both probes, and no staining was observed with Fc alone, AP alone, or an EphB-Fc probe that recognized ephrins-B (Figures 1Bb, 1Bd, and 1Bf; data not shown).

Because synaptic sites occupy only a small fraction of the muscle fiber surface, persistent ephrin expression at or near adult synapses might escape detection. We therefore doubly labeled muscles with EphA5-Fc plus rhodamine- α -bungarotoxin, which binds to acetylcholine receptors and thereby marks synaptic sites. Levels of ephrin-A were no higher at synaptic sites than elsewhere in neonatal muscle, and no ephrin was detectable at adult synapses (Figures 1Bh and 1Bi; data not shown).

In adults, motor axons can innervate denervated muscle but cannot hyperinnervate normal muscle. We therefore tested whether ephrin expression increased following denervation, as is known to be the case for some other recognition molecules, such as N-CAM (Covault and Sanes, 1985) and N-cadherin (Hahn and Covault, 1992). Levels of sarcolemmal ephrin increased markedly following denervation of neonates (Figure 1Bj). Ephrin levels also increased following denervation of adult muscle, albeit less markedly (data not shown). Interestingly, the positional selectivity of reinnervation is greater in neonates than in adults (Laskowski and Sanes, 1988; Laskowski and High, 1989).

Differential Sensitivity of Motor Axons to Ephrin-A5

Ephrins-A inhibit neurite outgrowth from many neuronal types (Flanagan and Vanderhaeghen, 1998), including spinal motoneurons (Donoghue et al., 1996; Ohta et al., 1997; Wang and Anderson, 1997; see Figure 2A). If ephrins regulate the establishment of neuromuscular topography, motoneurons from rostral and caudal spinal levels might be differentially sensitive to them. We tested this possibility in two ways.

First, we plated slices of cervical (rostral) or lumbar (caudal) spinal cord on membranes from fibroblasts that had been transfected with an ephrin-A5 expression vector (Donoghue et al., 1996). Nearly all of the neurites that emanate from such explants are derived from motoneurons (Wang et al., 1999). As shown in Figure 2B

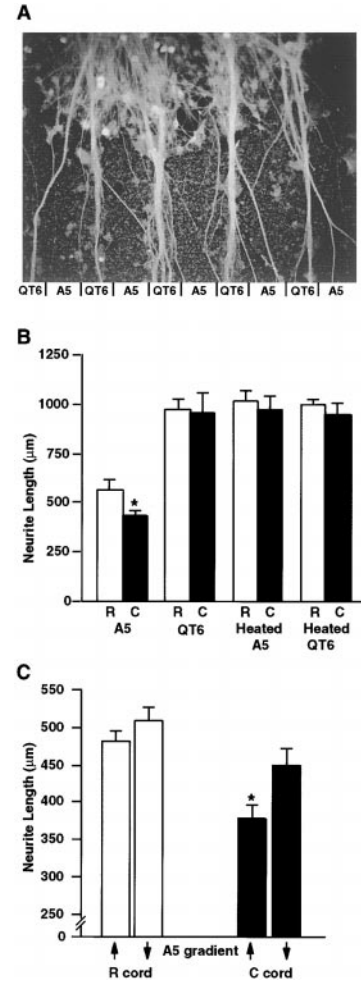


Figure 2. Rostral and Caudal Motoneurons Differ in Their Sensitivity to Ephrin-A5

Explants of cervical (rostral) or lumbar (caudal) spinal cord were plated on membrane-coated filters, and growth of neurites was assessed 3 days later. Nearly all neurites are derived from motoneurons under these conditions.

(A) Neurites on alternating lanes of membranes from control and ephrin-A5-transfected fibroblasts. When confronted with alternating lanes of membranes from control (QT6) and ephrin-A5-expressing (A5) fibroblasts, neurites grew preferentially on the former.

(B) Neurite length on filters coated with membranes from untransfected or ephrin-A5-expressing QT6 cells. Outgrowth was inhibited by ephrin-A5, but explants from rostral (R) spinal cord showed less inhibition than did explants from caudal (C) spinal cord (asterisk, difference between R and C is significant by Student's *t* test, $p < 0.05$). R and C neurites grew equal lengths on control membranes or on membranes in which ephrin-A5 had been inactivated by heating.

(C) Neurite outgrowth along gradients of increasing and decreasing ephrin-A5 concentration. Gradients were prepared as described by Baier and Bonhoeffer (1992). Neurites from rostral cord grew nearly equal distances up (↑) or down (↓) the gradient, although growth in both directions was less than that measured on ephrin-free control membranes (data not shown; see [B]). Neurites from caudal spinal cord were not only more sensitive to ephrin than were those from rostral cord but also were better able to discriminate increasing from decreasing ephrin concentrations (asterisk, difference between ↑ and ↓ is significant, $p < 0.01$).

Bars in (B) and (C) show mean \pm SE of measurements from 13–30 (B) or 67–72 (C) explants.

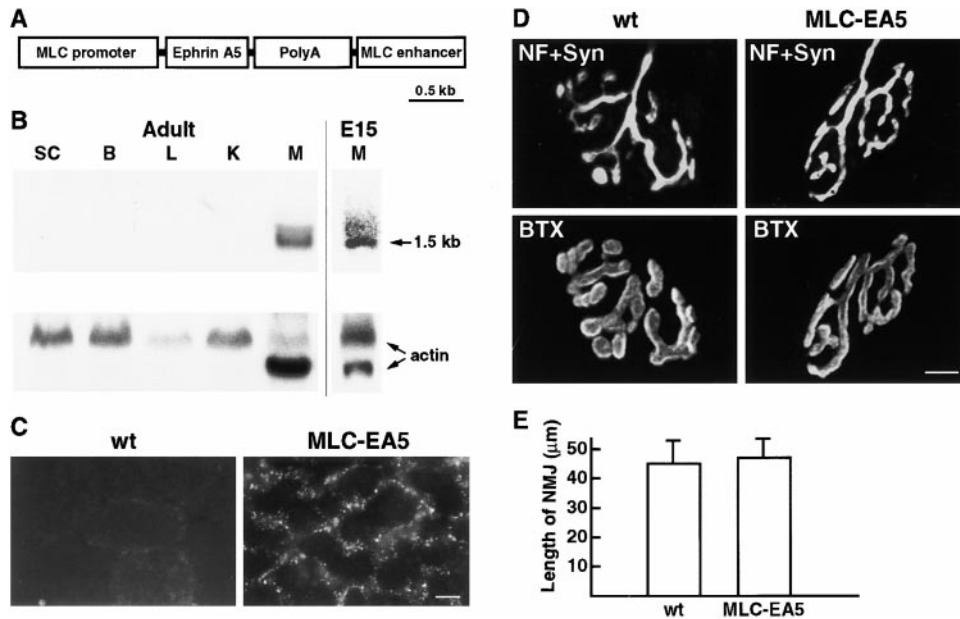


Figure 3. Forced Expression of Ephrin-A5 on Muscle Fibers in Transgenic Mice
 (A) Diagram of the transgene, in which ephrin-A5 is flanked by promoter and enhancer from the MLC 1f/3f gene to drive strong, muscle-specific expression. Scale bar, 0.5 kb.
 (B) Northern analysis of ephrin-A5 expression in spinal cord (SC), brain (B), liver (L), kidney (K), and hindlimb muscle (M) of adult MLC-EA5 transgenic mice and in muscle of E15 transgenic mice. Transgene expression is confined to muscle (top). The blots were reprobed with an actin cDNA, which hybridizes to cytoplasmic actin in all tissues as well as to sarcomeric actin in muscle (bottom).
 (C) Sections of adult gluteus muscle from wild-type (wt) and transgenic (MLC-EA5) mice stained with EphA5-Fc fusion. The transgene-encoded ephrin was expressed on muscle fiber surfaces. Scale bar, 20 μm.
 (D) Neuromuscular junctions from gluteus muscles of wild-type and MLC-EA5 mice, doubly stained to show pre- and postsynaptic specializations (antibodies to neurofilaments [NF] plus synaptophysin [Syn] and rhodamine-α-bungarotoxin [BTX], respectively). Synaptic structure was not detectably affected by ephrin-A5 overexpression. Scale bar, 10 μm.
 (E) Length of neuromuscular junctions, measured from sections such as those shown in (D). Ephrin-A5 expression had no significant effect on synaptic size. Bars show mean ± SD, n = 50 junctions of each genotype.

(first pair of bars), neurites from caudal explants were significantly shorter than those from rostral explants ($p < 0.05$). In contrast, outgrowth from both types of explants was equivalent on control (ephrin-free) membranes and on membranes in which ephrins had been inactivated by heating (Walter et al., 1987b). Thus, whereas ephrin-A5 inhibits outgrowth from both rostral and caudal motoneurons, the caudally derived population is on average more sensitive than is the rostral population.

Second, we used the method of Baier and Bonhoeffer (1992) to form shallow gradients of ephrin-A5-rich membranes, placed rostral or caudal spinal cord slices at the midpoint of the gradient, and measured neurite outgrowth in both directions (Figure 2C). As expected, outgrowth was inhibited with respect to that measured on ephrin-free membranes (compare Figures 2B and 2C), and inhibition was greater for caudal than for rostral neurites. Importantly, however, neurites from caudal explants grew significantly further in the direction of decreasing ephrin concentration than in the direction of increasing concentration, whereas rostral neurites were relatively insensitive to the direction of the gradient. The difference in length in the two directions was ~20% for neurites growing from caudal explants ($449 \pm 22 \mu\text{m}$ down the gradient versus $378 \pm 19 \mu\text{m}$ up the gradient, $p < 0.01$ by Student's *t* test) but only 5% for rostral neurites ($508 \pm 18 \mu\text{m}$ down the gradient versus $481 \pm 13 \mu\text{m}$ up the gradient, $p > 0.2$). Thus, caudal neurites

are better able than are rostral neurites to detect differences in ephrin concentration.

Disrupted Neuromuscular Topography in Muscles that Overexpress Ephrin-A5

To assess responses of motor axons to muscle-derived ephrins *in vivo*, we generated transgenic mice in which ephrin-A5 was selectively overexpressed in muscle fibers (Figure 3A). We used regulatory elements from the myosin light chain (MLC) 1f/3f chain gene for this purpose because they promote high levels of transgene expression in skeletal muscle fibers but are not detectably expressed in nonmuscle tissues or in nonmuscle cells within skeletal muscles (Rosenthal et al., 1989; Donoghue et al., 1991b). In addition, these regulatory elements promote graded expression among muscles, with 10- to 50-fold higher levels in hindlimb muscles than in thoracic muscles, including respiratory muscles (Donoghue et al., 1991a; Rao et al., 1996). Thus, even if ephrin overexpression impaired neuromuscular connectivity, we hoped to avoid lethality.

One transgenic line (called MLC-EA5) was selected for detailed study. Northern analysis confirmed selective expression of the transgene in MLC-EA5 skeletal muscle (Figure 3B). Expression was robust in embryos, when synapses form, and no expression was detectable in spinal cord. Staining with EphA5-Fc confirmed that ephrin was associated with muscle fiber membranes in

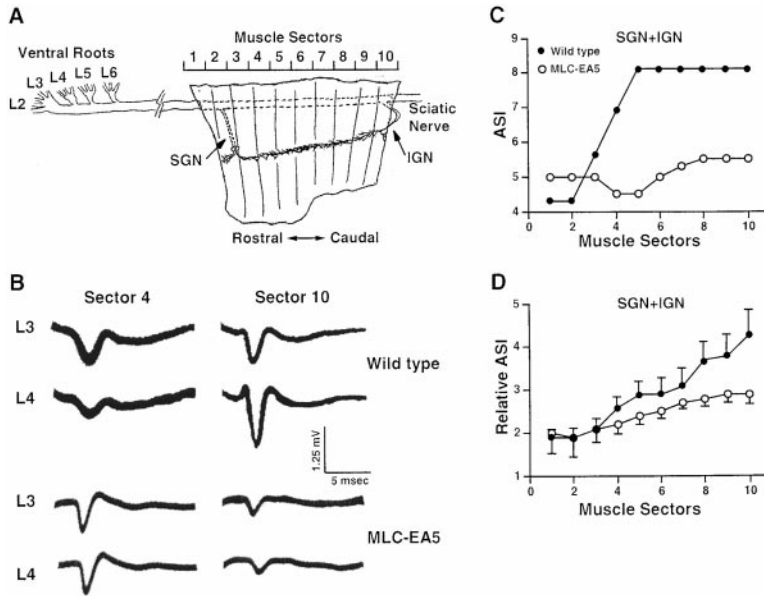


Figure 4. Ephrin-A5 Overexpression in Muscle Degrades Neuromuscular Topography

(A) Diagram of the gluteus muscle, showing its division into ten sectors, proceeding from the rostral to the caudal edge. The muscle is innervated by axons that enter the sciatic nerve through lumbar roots 2–6, then exit through the SGN and IGN and form a central endplate band on the muscle.

(B) Compound action potentials recorded from sectors 4 and 10 of wild-type and MLC-EA5 gluteus upon stimulation of L3 or L4. In wild-types, L3 and L4 selectively activated rostral and caudal sectors, respectively (L3:L4 = 1.8 in sector 4 and 0.53 in sector 10). This bias was absent from transgenic muscle (L3:L4 = 0.94 in sector 4 and 1.09 in sector 10).

(C and D) Topographic innervation of the wild-type gluteus (closed circles) and degradation of topography in MLC-EA5 gluteus (open circles). (C) shows a single muscle of each genotype, and (D) shows average values (\pm SE) from seven wild-type and seven MLC-EA5 muscles. In each case, groups of ventral rootlets were stimulated in turn, and localized

contractile responses were recorded from each muscle sector. The ASI was then calculated from each sector as described in the Experimental Procedures. Briefly, the lower the ASI, the more rostral the subset of motor axons that innervated the sector.

MLC-EA5 mice and absent from other intramuscular cells (Figure 3C). Ephrin levels varied among fibers within the muscle, but no consistent regional differences were observed (data not shown). The animals displayed no obvious abnormalities, and neuromuscular junctions were not detectably abnormal in size or shape (Figures 3D and 3E).

We chose the gluteus muscle for physiological analysis because it is a caudal muscle and because Brown and Booth (1983) showed previously that its motor pool is mapped systematically into its surface. The motor axons that innervate the gluteus arise in lumbar (L) segments L2–L6, exit the spinal cord through the corresponding lumbar roots, and travel through the hindlimb in the sciatic nerve. Some gluteal motor axons exit the sciatic through the superior gluteal nerve (SGN), which enters the muscle near its rostral edge, while the remainder exit through the inferior gluteal nerve (IGN) to enter the muscle from the caudal edge. Axons from both nerves then travel perpendicular to the muscle fibers, forming a single endplate band near the center of the muscle (Figure 4A). We dissected lumbar spinal nerves L1–L6, the sciatic nerve, the SGN and IGN, and the gluteus muscle in continuity and used small pins to demarcate ten equal sized sectors of the muscle. We then stimulated ventral roots or groups of ventral rootlets and determined which sectors of the muscle they innervated. This determination was made either by recording compound muscle action potentials from individual sectors with an extracellular electrode or by mapping localized contractile responses within individual sectors.

Both methods showed that the rostrocaudal axis of the gluteus motor pool is mapped onto the rostrocaudal axis of the muscle in wild-type mice and revealed that this map is dramatically degraded in MLC-EA5 mice. For example, stimulation of L3 evoked a larger compound action potential in muscle sector 4 of a wild-type mouse than did stimulation of L4 (L3:L4 = 1.8), whereas the

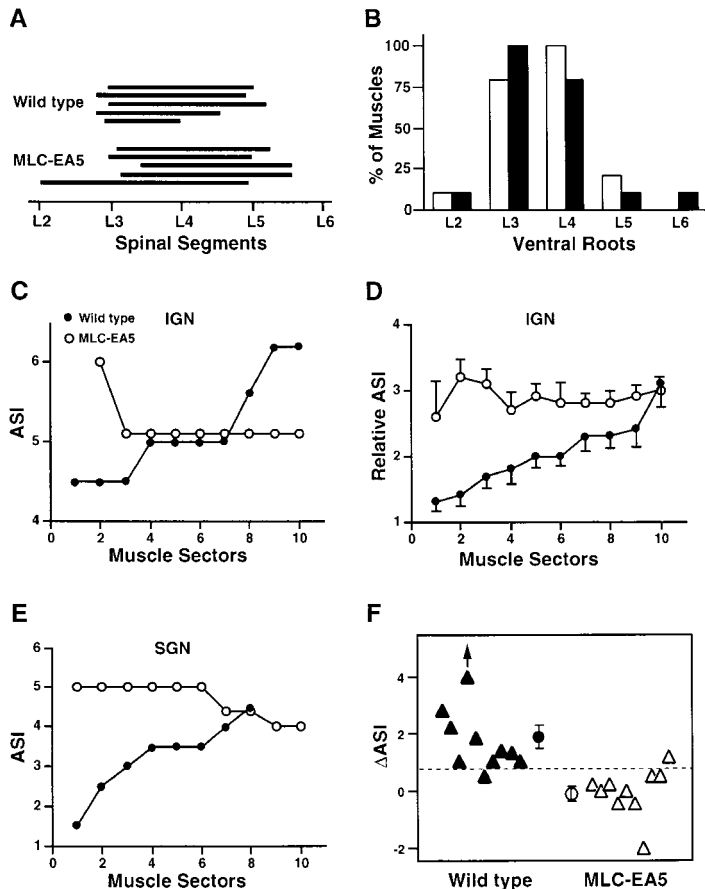
reverse was true in caudal muscle sector 10 (L3:L4 = 0.53; Figure 4B). In the MLC-EA5 muscle, in contrast, stimulation of L3 and L4 evoked similar sized responses from all segments (for example, L3:L4 = 0.94 in sector 4 and 1.09 in sector 10). Likewise, measurement of local contractions showed that successively more caudal portions of the motor pool innervated successively more caudal sectors of the wild-type muscle, whereas the segmental origin of inputs varied little among sectors in the MLC-EA5 muscle (Figure 4C).

To permit comparison among animals and genotypes, we calculated an average segmental innervation (ASI) for each muscle sector, as detailed previously (Wigston and Sanes, 1982, 1985; Laskowski and Sanes, 1987, 1988). Briefly, the lower the ASI, the more rostral the subset of axons that innervated the sector. Using this index, the difference between wild-type and transgenic muscles was consistent and significant in this series of experiments (Figure 4D), and topography was virtually abolished in a separate set of experiments described in the next section. Thus, overexpression of ephrin-A5 in the gluteus muscle impairs the ability of the motor nerve to form an intramuscular topographic map of synaptic connectivity.

Locus of the Neuromuscular Defect in Ephrin-A5-Overexpressing Mice

Ephrin-A5 overexpression in muscle fibers could perturb neuromuscular topography by affecting target recognition or synaptic stability. However, alterations in topography could also be indirect consequences of nonsynaptic effects. For example, the position of the motor pool might be altered, axons might make aberrant choices in entering the SGN or IGN, or the geometry of the intramuscular nerve might be affected. We undertook a series of experiments to test these alternatives.

First, we determined the rostrocaudal position of gluteus motor neurons by retrograde labeling from the muscle. In both wild-type and MLC-EA5 transgenic mice,



(F) Data from experiments shown in (D) are replotted to show the difference between the ASI of the two rostralmost and the two caudalmost sectors in each muscle. This plot shows that topography was present in all wild-type mice ($\Delta\text{ASI} > 0$ in all ten muscles; mean $\Delta\text{ASI} = +1.9$) and was almost completely lost in MLC-EA5 mice (mean $\Delta\text{ASI} = -0.04$). The dotted horizontal line emphasizes the consistent difference between groups. These results eliminate the possibility that topography in wild types and/or abolition of topography in MLC-EA5 mice resulted from axonal choices within the sciatic nerve.

the gluteus motor pool was centered at the level of emergence of the L4 ventral root and extended from approximately the L3 to the L5 root (Figure 5A). Neither the rostrocaudal extent of the pool nor the apparent number of neurons in it differed between wild-type and transgenic mice. Thus, alterations in the position of the motor pool neither resulted from nor led to alteration in intramuscular topography in MLC-EA5 transgenic mice.

Next, we asked whether axonal choices within the sciatic nerve were responsible for topography in the wild-type gluteus or for its disruption in MLC-EA5 mice. For example, more rostrally derived motor axons might be specified to exit the sciatic through the SGN in wild types and thereby innervate the rostral part of the muscle. If this were the case, altered sorting of gluteus motor axons in the sciatic nerves of MLC-EA5 mice could impair topography. To test these possibilities, we cut either the SGN or the IGN before assessing contractile responses so that we could determine the projection pattern of axons that entered the muscle through a single nerve. In wild-type mice, axons that entered through each nerve formed an orderly map onto the gluteus, indicating that axonal choices within the sciatic nerve are not responsible for (although they may influence) neuromuscular topography. Moreover, maps formed by

Figure 5. Ephrin-A5 Overexpression in Muscle Does Not Affect the Rostrocaudal Extent of the Gluteus Motor Pool or the Choices of Motor Axons in the Sciatic Nerve

(A) Motor pools were mapped by retrograde transport following injection of a fluorescent dye into the gluteus. Each horizontal line represents one animal. In both wild-type and MLC-EA5 mice, the gluteus motor pool extended from near the L3 to near the L5 ventral root.

(B) Ventral roots containing axons that innervated wild-type (open bars) and MLC-EA5 (black bars) gluteus muscles through the IGN. These data were obtained from the experiments summarized in Figure 5D. Transgene expression had no detectable effect on the complement of axons that exit the sciatic nerve through the IGN.

(C and D) Topographic innervation of the wild-type gluteus (closed circles) and degradation of topography in MLC-EA5 gluteus (open circles) by axons that run through the IGN. In these experiments, the SGN was cut before stimulating and recording. (C) shows a single muscle of each genotype, and (D) shows average values (\pm SE) from ten wild-type and ten MLC-EA5 muscles. Innervation was topographically biased in wild-type mice, and topography was almost entirely abolished in MLC-EA5 mice.

(E) Topographic innervation of the wild-type gluteus (closed circles) and degradation of topography in MLC-EA5 gluteus (open circles) by axons that run through the SGN. This experiment was similar to that shown in (C), except that the IGN was cut before recording.

both SGN and IGN axons were disrupted in MLC-EA5 mice (Figures 5C and 5E).

Because projections through a single nerve are uncontaminated by axonal choices within the sciatic, we reexamined the effects of ephrin overexpression on neuromuscular topography by assaying maps formed through the IGN in a series of ten wild-type and ten MLC-EA5 mice. As shown in Figure 5D, axons entering the gluteus through the IGN showed virtually no positional bias in MLC-EA5 mice. To judge how consistent this effect was, we compared the ASI of the two rostralmost and two caudalmost sectors from each muscle (Figure 5F). This difference was positive in all ten wild-type muscles (mean = 1.9), abolished in MLC-EA5 muscles (mean = -0.04), and greater in nine of ten wild-type muscles than in any but one of the ten MLC-EA5 muscles (dotted line in Figure 5F). Thus, the choices of axons at exit points from the sciatic nerve can explain neither topographic mapping in normal muscles nor disruption of the map in the mutant.

As an additional means of testing the possibility that transgene expression affected axonal choices within the sciatic, we asked which ventral roots innervated the gluteus through the IGN. In fact, there was no marked difference between the segmental origin of inputs to the

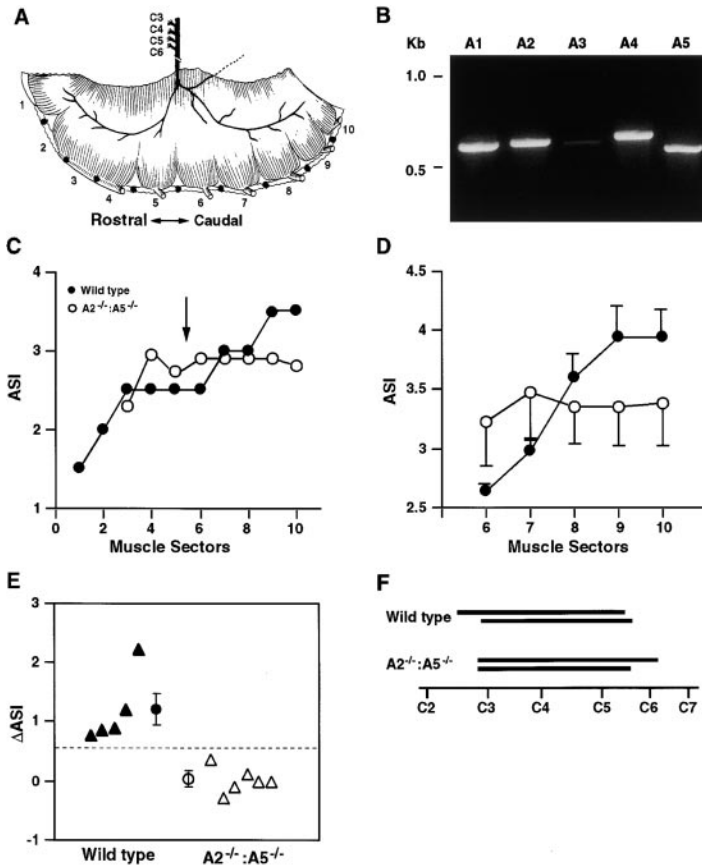


Figure 6. Degraded Neuromuscular Topography in the Diaphragm Muscle of *ephrin-A2^{-/-}:ephrin-A5^{-/-}* Mice

(A) Diagram of the diaphragm muscle, showing its division into ten sectors, proceeding from the rostral/ventral to the caudal/dorsal edge. The muscle is innervated by axons that leave the spinal cord from cervical roots 3–6, run through the phrenic nerve, enter the hemidiaphragm centrally, and then form central intramuscular nerves in each quadrant.

(B) RT-PCR analysis of expression of ephrins-A1–A5 in E15 diaphragm. Like other muscles (see Figure 1), the diaphragm expresses ephrins-A.

(C and D) Neuromuscular topography in wild-type (closed circles) and *ephrin-A2^{-/-}:ephrin-A5^{-/-}* (open circles) diaphragm, calculated as described in the Experimental Procedures and the Figure 4 legend. (C) shows a whole hemidiaphragm from a single animal of each genotype, and (D) shows average values of sectors in the caudal quadrant from six wild-type and six *ephrin-A2^{-/-}:ephrin-A5^{-/-}* muscles. In the wild-type, successively more caudal segments were innervated by successively more caudally derived subsets of motor axons (see also Laskowski and Sanes, 1987, 1988). In the mutant, the topography of innervation was degraded, and no topographic bias was detectable in the caudal quadrant.

(E) Data from experiments shown in (D) are replotted to show the difference between the ASI of the two rostralmost and two caudalmost sectors in each muscle. This plot shows that topography was consistent in wild-type mice ($\Delta\text{ASI} > 0.75$ in all five muscles) and was almost completely lost in *ephrin-A2^{-/-}:ephrin-A5^{-/-}* mice (mean $\Delta\text{ASI} = 0.01$). The dotted line emphasizes the difference between the two groups.

(F) Motor pools of wild-type and *ephrin-A2^{-/-}:ephrin-A5^{-/-}* diaphragm mapped by retrograde transport following injection of a fluorescent dye into the muscle. Each horizontal line represents one animal. The position of the motor pool was not detectably affected in the mutant.

IGN between wild-type and MLC-EA5 mice (Figure 5B). We do not conclude, however, that axonal choices at exit points are random, only that they are unaffected by ephrin overexpression in muscle. Indeed, the residual topography seen in the initial set of experiments on MLC-EA5 mice (compare Figures 4D and 5D) may reflect slight preferences of rostrally and caudally derived axons to exit the sciatic nerve through the SGN and IGN, respectively.

Finally, we asked whether overexpression of ephrin-A5 affected the branching pattern of the intramuscular nerves or the extent to which either the SGN or the IGN extended across the surface of the muscle. No significant differences were detected between wild-type and MLC-EA5 mice either in the overall branching patterns or in the territories innervated by either nerve branch (data not shown). Taken together with the selective expression of the transgene in muscle fibers, these results provide strong evidence that ephrin-A5 overexpression disrupts the neuromuscular map at the synaptic level.

Neuromuscular Defects in Mice Lacking Ephrins-A2 and -A5

Results from MLC-EA5 mice show that exogenous ephrins can affect synapses. To ask whether endogenous ephrins are involved in the establishment of neuromuscular topography, we examined muscles of mice

bearing targeted mutations of the *ephrin-A2* or *ephrin-A5* genes, or double mutants lacking both ephrins. The majority of homozygous single mutants (*ephrin-A2^{-/-}* or *ephrin-A5^{-/-}*) are viable and fertile but have defective retinocollicular and retinogeniculate projections; double mutants (*ephrin-A2^{-/-}:ephrin-A5^{-/-}*) are also outwardly normal but show more severe defects in the organization of the retinocollicular projection than does either single mutant (Feldheim et al., 1998; Frisen et al., 1998; D. F. et al., unpublished data). A detailed analysis of neuromuscular relationships in single and double mutants will be presented elsewhere, and pertinent data from *ephrin-A5^{-/-}* muscles are presented below; here, we focus on the *ephrin-A2^{-/-}:ephrin-A5^{-/-}* diaphragm, chosen because we have previously studied the topography of its innervation in detail (Laskowski and Sanes, 1987, 1988; Laskowski and Owens, 1994).

The diaphragm is innervated through the paired phrenic nerves, which travel through the thorax carrying axons that arise through cervical roots C3–C6. Each nerve enters the ipsilateral hemidiaphragm near its midpoint, then bifurcates to form intramuscular branches that innervate the rostral and caudal quadrants (Figure 6A). Most axons that arise from the rostral portion of the motor pool (C3 and C4) enter the rostral intramuscular branch, whereas caudally derived axons (from C5 or C6) enter the caudal branch. In addition, within each

quadrant, the rostrocaudal axis of the motor pool is topographically mapped onto the rostrocaudal axis of the muscle. Together, the segregation of axons at the main branchpoint and the intramuscular maps within each quadrant give rise to an orderly topographic map that extends along the entire hemidiaphragm (Laskowski and Sanes, 1987). The embryonic diaphragm, like other muscles, expresses ephrins-A (Figure 6B).

Innervation was assessed as described above for MLC-EA5 muscles. The muscle was divided into sectors, based on the association of fibers with successive ribs (Laskowski and Sanes, 1987); ventral roots C3–C6 were stimulated separately, and inputs to each sector were noted. As we showed previously for rat, the rostrocaudal axis of the phrenic motor pool was mapped onto the surface of the diaphragm in wild-type mice. This mapping was impaired in *ephrin-A2^{-/-}:ephrin-A5^{-/-}* double mutants (Figure 6C). Axons appeared to make appropriate choices between the rostral and caudal intramuscular nerve branches as they entered the diaphragm (data not shown), but they did not form appropriate maps within each quadrant (Figure 6D). Comparison of the ASI of the two rostralmost and two caudalmost sectors from the caudal quadrant of each muscle (as detailed above for gluteus) confirmed that the difference was a consistent one: the difference was greater in all six of the double mutant diaphragms tested than in any of the five control diaphragms (dotted line in Figure 6E). Thus, loss and gain of ephrin function both perturb neuromuscular topography.

We used retrograde labeling to determine whether loss of ephrins-A2 and -A5 affected the position of the phrenic (diaphragm) motor pool. The pool extended from the levels of the C3 to the C6 ventral root in both controls and *ephrin-A2^{-/-}:ephrin-A5^{-/-}* mutants, with no apparent difference between genotypes (Figure 6F). Likewise, intradiaphragmatic nerve branching patterns and the size and shape of neuromuscular junctions did not differ detectably between controls and double mutants (data not shown). Thus, loss of ephrins is likely to impair neuromuscular matching by an intramuscular mechanism.

Altered Motor Pool in Mice Lacking Ephrin-A5

As part of our survey of nerve–muscle topography in ephrin mutants, we recorded from the acromiotrapezius. Acromiotrapezius muscle fibers run mediolaterally from the median raphe of the neck to the scapular spine (Figure 7A) and can be divided into a series of eight rostrocaudally arrayed sectors. Initial studies showed that motor axons innervating the acromiotrapezius exit the central nervous system through the spinal accessory nerve (cranial nerve XI) and the rostralmost cervical ventral roots; the inputs from the cervical spinal roots join to form a single connective that then fuses with the spinal accessory nerve, forming a single nerve that enters the muscle.

All sectors of the acromiotrapezius in both controls and mutants were innervated by axons from both the spinal accessory nerve and the cervical connective. However, a distinct subset of low threshold motor axons that ran through the cervical connective (revealed by stimulation at low voltage) displayed distinct preferences in mutants and controls. These axons innervated

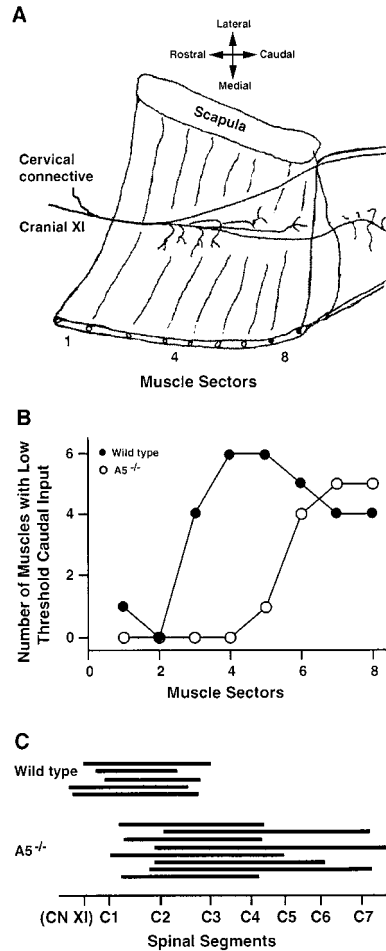


Figure 7. Altered Inputs to and Topographic Innervation of the Acromiotrapezius Muscle in *ephrin-A5^{-/-}* Mice

(A) Diagram of the acromiotrapezius muscle, showing its division into eight sectors, proceeding from the rostral to the caudal edge. The muscle is innervated by axons that run through cranial nerve XI and a caudal connective derived from the uppermost cervical roots.

(B) Innervation of six wild-type (closed circles) and five *ephrin-A5^{-/-}* acromiotrapezius muscles by low-threshold motor axons running through the caudal connective. This subpopulation of caudally derived axons innervated all but the rostralmost quarter of control muscles but only the caudalmost sectors of *ephrin-A5^{-/-}* muscles.

(C) Motor pools of wild-type and *ephrin-A5^{-/-}* acromiotrapezius, mapped by retrograde transport following injection of a fluorescent dye into the muscle. Each horizontal line represents one animal. The motor pool was longer and also shifted caudally in the mutant.

all but the two rostralmost sectors of control muscles, but they passed over five rostral segments in mutant muscles, to innervate only the three caudalmost sectors (Figure 8B). The caudalward shift caused by loss of ephrin-A5 therefore covered nearly half of the muscle (that is, three of eight sectors).

As described above for the gluteus and diaphragm, we used retrograde labeling to locate the acromiotrapezius motor pool. In control mice, this pool extended from the caudalmost portion of the brainstem to the third cervical segment of the spinal cord (Figure 8C, top). In *ephrin-A5^{-/-}* mutants, the motor pool occupied a similar position in the dorsoventral plane (data not shown) but was

altered in two ways (Figure 8C, bottom). First, mutant motor pools extended over more segments than did wild-type motor pools—an average of about 2.5 segments in controls and about 4 in mutants. Second, the pool was shifted caudalward in mutants. Thus, even though the mutant motor pools were longer than were control pools, all five wild-type pools tested extended further rostrally than did any of the eight mutant pools. Likewise, all eight mutant motor pools examined extended further caudally than did any wild-type pool. This result suggests that ephrins can affect neuromuscular connectivity by intraspinal as well as intramuscular mechanisms.

Discussion

The aim of the studies reported here was to assess the possibility that ephrins affect positionally selective synapse formation between motor axons and muscle fibers. Our main results are as follows. First, developing muscles express all five known *ephrin-A* genes. Second, levels of two ephrin-A RNAs (A1 and A5) are higher in rostral than in caudal muscles. Third, developing and denervated muscle fibers, which are susceptible to innervation, bear ephrins-A on their surfaces, whereas adult muscle fibers, which are refractory to innervation, do not. Fourth, ephrins-A are present at synaptic sites on myotubes, although they are not confined to those sites. Fifth, caudally derived (lumbar) motor axons are more sensitive than are rostrally derived (cervical) motor axons to ephrins. Sixth, selective overexpression of *ephrin-A5* in muscle fibers markedly degrades the topographic mapping of gluteus motor axons onto the gluteus muscle. Seventh, topographic mapping is also defective in diaphragms of mutant mice that lack *ephrin-A2* and *ephrin-A5*. Taken together, these results support the hypothesis that muscle-derived ephrins bias neuromuscular synapse formation in favor of positionally matched partners.

Because ephrins are expressed by numerous cell types besides myotubes, perturbing their expression might perturb neuromuscular topography by indirect means. For example, Eph kinase–ephrin interactions have been implicated in tract formation within the spinal cord (Park et al., 1997; Dottori et al., 1998); patterning of somites, from which muscles arise (Durbin et al., 1998); migration of neural crest, from which Schwann cells arise (Krull et al., 1997); and initial outgrowth of motor axons into the periphery (Wang and Anderson, 1997). Moreover, the position of at least one motor pool—that of the acromiotrapizeus muscle—is shifted in *ephrin-A5* mutant mice, indicating that loss of ephrins affects neuromuscular connectivity by intraspinal mechanisms. It was therefore important to critically examine the idea that ephrins are directly involved in nerve–muscle matching. We believe this is the case for several reasons. First, ephrin overexpression is confined to muscle fibers in MLC-EA5 transgenic mice, which display a striking defect in nerve–muscle topography. Second, this defect occurs without any detectable effect on the position of the motor pool or on the choices that axons make on their way from the spinal cord to the muscle.

Third, defective topography in the diaphragms of *ephrin-A2^{-/-}:ephrin-A5^{-/-}* double mutants occurs in the absence of any detectable effect on the location of the phrenic motor pool or the structure of the phrenic nerve.

If we accept the conclusion that ephrins are directly involved in nerve–muscle matching, new questions arise about how they act. These can be divided into issues of mapping and synaptogenesis. In terms of mapping, one plausible model is that muscle fibers express different levels or combinations of ephrins in accordance with their positions and that motor axons express different levels or combinations of Eph kinases (the likely ephrin receptors) in accordance with their positions. For example, levels of expression might be graded along the rostrocaudal axis, as appears to be the case in the retinotectal system. Alternatively, patterns of ephrin and Eph kinase expression might describe a more complex combinatorial code (Kilpatrick et al., 1996; Ohta et al., 1996; Araujo et al., 1998), as suggested by the discrete identities of motor pools and muscles. Indeed, whereas Eph kinase and ephrin levels are graded along the rostrocaudal axis in the visual system, there is currently no evidence for graded expression of ligands or receptors in the motor system. Another possibility is that interactions between ephrins and their receptors are permissive rather than instructive, enabling positional information to be transmitted by other molecules. It is important to emphasize that our data do not distinguish permissive versus instructive roles of ephrins.

Disappointingly, data needed to decide among these alternatives are not yet available. First, our data on expression reflect intermuscular differences rather than intramuscular differences. The low abundance of ephrin RNA has made it infeasible to map intramuscular variations in ephrin expression by *in situ* hybridization (see Donoghue et al., 1996). Appropriate antibodies are not available, and the EphA5–Fc and EphA3–AP fusions do not distinguish among the ephrins-A. Similarly, culture methods are not yet sufficiently refined to permit assessment of variable sensitivity to ephrins within a motor pool. Second, the transgenic and mutant strains we generated required that we assess consequences of gain and loss of function in different muscles. No changes in the topographic innervation of the gluteus muscle were detectable in the mutants, perhaps because ephrins are expressed at higher levels in rostral than in hindlimb muscles (Donoghue et al., 1996; Figure 1A). Conversely, no changes in topography of diaphragm were detectable in MLC-EA5 mice, presumably because the MLC promoter drives low levels of transgene expression in this muscle (Donoghue et al., 1991a). Third, further studies will be required to determine how the distribution of Eph kinases varies among motor axons. Finally, it will be necessary to incorporate evidence that muscles express Eph kinases as well as ephrins and that cells of the spinal cord express ephrins as well as Eph kinases (Gale et al., 1996; Kilpatrick et al., 1996; Araujo et al., 1998); this complexity raises the possibility that Eph kinases and ephrins interact in *cis* as well as in *trans* (Hornberger et al., 1999).

Whatever the distribution of the ephrins, their involvement in the neuromuscular system provides an opportunity to learn how they affect individual synapses. Some of the intercellular signals that regulate synaptogenesis

at the neuromuscular junction have now been identified; these include neuregulins, agrin, and laminins (reviewed by Sanes and Lichtman, 1999). These signals, and their signal transduction apparatus, appear to be shared by all neuromuscular junctions, consistent with the generalization that any motor axon is capable of forming a mature functional synapse on any skeletal muscle fiber. Yet, synaptogenesis is a selective process, with a bias in favor of positionally matched partners. In this regard, it is interesting that ephrins are present at sites of developing neuromuscular junctions (Figure 1), as also appears to be the case at central synapses (Torres et al., 1998; Bruckner et al., 1999; Buchert et al., 1999). Ephrins might interact with shared signals to modulate their efficacy (see, for example, Huynh-Do et al., 1999). Such modulation could affect the probability that a nerve-muscle contact is synaptogenetically productive, make a favored synapse stronger, or confer a competitive advantage on appropriate synapses in the interactions that lead to synapse elimination. Alternatively, variations in ephrin level within (or between) muscles might exert local effects on motor axons, regulating terminal branching and thereby affecting the probability of synapse formation. Comparison of synaptic development in muscles of control and MLC-EA5 mice should provide a way to distinguish among these possibilities.

Finally, analysis of *ephrin-A5*^{-/-} mutants provided evidence that ephrins can affect neuromuscular topography by intraspinal as well as intramuscular mechanisms: the motor pool of the acromiotrapezius was elongated and shifted caudally in these mutants. In fact, Eph kinase-ephrin interactions may affect circuitry within the spinal cord in multiple ways, in that *EphA4* and *EphA8* mutant mice also show spinal defects (Park et al., 1997; Dottori et al., 1998). The mechanism by which loss of ephrin-A5 leads to an alteration in the motor pool is completely unknown—it is equally possible that motoneurons are incorrectly specified in the mutant or that they are correctly specified but misrouted within or after exiting the spinal cord. It is interesting to speculate, however, that the defect we observe is related to the alterations in the positions of motor pools observed in mutant mice lacking the *Hoxc-8* or *Hoxd-10* genes (Carpenter et al., 1997; Tiret et al., 1998). The finding that *Hox* genes regulate Eph kinase expression in the hindbrain (Studer et al., 1998) is consistent with this possibility. We therefore suggest that Eph kinases and ephrins are components of the molecular machinery by which *hox*-encoded information about axial position is converted into guidance cues that pattern the peripheral nervous system.

Experimental Procedures

Animals

Ephrin-A5^{-/-} mutant mice were generated by gene targeting as described previously (Frisen et al., 1998). Generation of *ephrin-A2*^{-/-} null mutant mice will be described elsewhere (D. A. F. and J. G. F., unpublished data). Double mutants were obtained by breeding the single mutants. Both of the single mutants and the double mutants were viable and fertile.

The transgene diagrammed in Figure 3 consisted of the human ephrin-A5 open reading frame (Donoghue et al., 1996) flanked by promoter and enhancer elements from the rat MLC 1f/3f gene (Rosenthal et al., 1989). These regulatory elements promote expression

in caudal skeletal muscle, but are not detectably expressed in non-muscle tissues, including nervous tissue (Donoghue et al., 1991a, 1991b; Rao et al., 1996). Transgenic mice were generated by injection of DNA into the fertilized oocyte, using standard techniques. Embryos for injection were obtained from matings between (C57BL6/J and CBA) F1 hybrids. Transgenic founders were subsequently backcrossed to C57BL6/J mice for one to four generations before use. Genotypes were determined by PCR, and wild-type littermates of transgenic or mutant mice were used as controls.

RNA Analysis

Poly(A)⁺ RNA was fractionated on formaldehyde-agarose gels, transferred to Genescreen Plus membrane (Dupont), and probed at high stringency with α -³²P-dCTP-labeled cDNA probes (random primed DNA labeling kit; Boehringer Mannheim). Following exposure to X-ray film, the blots were stripped and reprobed with cDNA for elongation factor EF-1 α .

For RT-PCR, total RNA was prepared from rostral (shoulder and forelimb), caudal (thigh and hindlimb), and diaphragm muscles of E16 mice. cDNA was then prepared with reverse transcriptase using oligo-dT as a primer. Primers were designed to specifically amplify ~500 nt fragments of ephrin-A1-A5 RNAs and a 1.5 kb fragment of EF-1 α RNA. Quantitative PCR was then performed by a modification of the methods of Freeman et al. (1994). Briefly, EF-1 α RNA was used to calibrate the amount of RNA in each sample, and cycle number was adjusted to be within the linear range of amplification. Once optimal conditions were determined, PCR was carried out in the presence of tracer amounts of α -³²P-dCTP. Products were separated on gels, and radioactivity was quantitated on a Phosphorimager.

Histochemistry

Ephrins were detected with fusion proteins consisting of either the extracellular domain of EphA5 fused to the Fc domain of human IgG heavy chain (Gale et al., 1996) or the extracellular domain of EphA3 fused to AP (Cheng et al., 1995). Cryostat sections (10–40 μ m) were incubated for 1 hr with fusion protein (30 μ g/ml), then washed with phosphate-buffered saline, fixed with formaldehyde, and reincubated with fluorescein-labeled rabbit anti-human IgG. In some experiments, the sections were counterstained with rhodamine- α -bungarotoxin (Molecular Probes), which binds to acetylcholine receptors in the postsynaptic membrane. Controls included Fc, EphB-Fc, and AP. The size and geometry of neuromuscular junctions were revealed by a whole-mount double-staining method described previously (Gautam et al., 1996).

Mapping Neuromuscular Topography

Neuromuscular topography was determined in 2- to 5-week-old animals. At younger ages, we were concerned that synapse elimination would not be complete, and at later ages thickening of the bone made dissection difficult. Animals were deeply anesthetized with ketamine and xylazine, perfused through the heart with Ringer solution (Laskowski and Sanes, 1987), and decapitated. Muscles were then dissected along with their nerves and ventral roots. For gluteus muscles, the lumbar spinal cord, its roots, the sciatic nerve, the SGNs and IGNS, and the muscle itself were dissected in continuity. The nerves and muscles were mounted ventral (deep) surface up and superfused with Ringer solution that was continually bubbled with oxygen. The points at which the superior and inferior nerves entered the muscle were used to define the rostral and caudal boundaries of the muscle. We divided the intervening area into ten equal "sectors" and inserted small, sharpened (minuten) pins along the medial margin of the muscle at borders between sectors (Figure 3A). Ventral roots L2–L5 were subdivided into bundles of rootlets and pulled into stimulating electrodes with gentle suction.

Patterns of innervation were assessed in two ways. The first was to record action potentials extracellularly from groups of muscle fibers. For this purpose, an insulated tungsten microelectrode (~1 M Ω , Frederick Haer) was gently pressed onto the surface of groups of muscle fibers in the center of a sector. Movements were minimized by stretching the muscle. Ventral roots were then stimulated in turn, and the resulting compound muscle action potentials were recorded on an oscilloscope. The surface electrode was then moved to another sector and the stimulation repeated. The amplitudes of

compound action potentials evoked in a single sector by maximal stimulation of rostral and caudal rootlets were compared.

The second method of assessing innervation pattern was to stimulate each group of rootlets in turn and note which sectors responded with a twitch. Although this method appears to be crude, we showed previously that calculations of topography obtained by visual detection of localized contractions correlate well with those derived by intracellular recording of synaptic potentials (Laskowski and Sanes, 1987). We used this method in most experiments because it permitted a more complete analysis of topography throughout the entire muscle than either the electromyographic or the intracellular methods. To display the data, each group of rootlets was assigned a number, with "1" being the most rostral that innervated any part of the muscle. The arithmetic mean of all groups of rootlets that innervated each muscle sector was then calculated. This value, used previously, is termed the "average segment of innervation" (Wigston and Sanes, 1982, 1985; Laskowski and Sanes, 1987, 1988). Because the rostralmost input differed among muscles within a group (for example, only a few of the gluteus muscles were innervated through L2; see Figure 5B), different inputs were numbered "1" in different muscles. We therefore use the term "relative ASI" for pooled data.

Acromiotrapezium and diaphragm muscles were assayed by similar methods. For the acromiotrapezium, the spinal accessory nerve (cranial nerve XI) and the cervical connective that joins it were maintained. The diaphragm was dissected along with the entire length of the phrenic nerve and roots C3–C6.

Mapping Motor Pools

The intraspinal position of motoneurons that innervated individual muscles was determined by retrograde labeling using fast blue dye (FB; 1 μ l of a 100 μ g/ml solution in 10% dimethyl sulfoxide) as described previously (Laskowski and Sanes, 1987). After 3–4 days, the muscle was dissected to confirm the accuracy of dye placement and to be sure that no surrounding muscles had been contaminated. Then the appropriate region of the spinal cord was dissected free of the vertebral column and sectioned longitudinally at 50 μ m. Positions of FB-labeled cells, all of which were identifiable as motoneurons, were recorded for each section. Finally, sections were aligned by positions of ventral roots, and the motor column was reconstructed.

Cultures

Cells of the quail fibroblast QT6 cell line were stably transfected with an *ephrin-A5* expression vector (Donoghue et al., 1996), and membranes were purified by sucrose density gradient centrifugation as previously described (Wang et al., 1999). The membrane fractions were then adjusted to 200 μ g/ml of protein and used to prepare stripes using the apparatus introduced by Walter et al. (1987a) or gradients using the apparatus of Baier and Bonhoeffer (1992).

Rostral (cervical) and caudal (lumbar) portions of spinal cords were isolated from E15 rat embryos and sectioned at 300 μ m. Slices of spinal cord were cultured on the membranes for 3 days, then fixed in 4% paraformaldehyde and stained with antibodies to neurofilaments (Wang et al., 1999). Neurite length was determined by measuring the distance from the edge of the ventral surface of the spinal cord slice to the leading edge of growing neurites. Three measurements from each explant were averaged to give a single value.

Acknowledgments

We thank Jeanette Cunningham, Mia Nichol, and Sherry Weng for assistance; Nick Gale and George Yancopoulos (Regeneron) for the generous gift of EphA5–Fc fusion protein; and Chris Henderson for comments on the manuscript. This work was supported by grants from the National Institutes of Health to J. R. S., M. B. L., and J. G. F. and a grant from the Muscular Dystrophy Association to J. R. S.

Received May 26, 1999; revised November 22, 1999.

References

Araujo, M., Piedra, M.E., Herrera, M.T., Ros, M.A., and Nieto, M.A. (1998). The expression and regulation of chick *EphA7* suggests roles in limb patterning and innervation. *Development* **125**, 4195–4204.

Baier, H., and Bonhoeffer, F. (1992). Axon guidance by gradients of a target-derived component. *Science* **255**, 472–475.

Bennett, M., and Ho, S. (1988). The formation of topographical maps in developing rat gastrocnemius muscle during synapse elimination. *J. Physiol.* **396**, 471–496.

Bennett, M.R., and Lavidis, N.A. (1984). Development of the topographical projection of motor neurons to a rat muscle accompanies loss of polyneuronal innervation. *J. Neurosci.* **4**, 2204–2212.

Brambilla, R., Bruckner, K., Orioli, D., Bergemann, A.D., Flanagan, J.G., and Klein, R. (1996). Similarities and differences in the way transmembrane-type ligands interact with the Elk subclass of Eph receptors. *Mol. Cell. Neurosci.* **8**, 199–209.

Brown, M.C., and Booth, C.M. (1983). Postnatal development of the adult pattern of motor axon distribution in rat muscle. *Nature* **304**, 741–742.

Browne, K.M. (1950). The spatial distribution of segmental nerves to striate musculature of the hindlimb of the rat. *J. Comp. Neurol.* **93**, 441–455.

Bruckner, K., Pablo-Labrador, J., Scheiffele, P., Herb, A., Seeburg, P.H., and Klein, R. (1999). EphrinB ligands recruit GRIP family PDZ adapter proteins into raft membrane microdomains. *Neuron* **22**, 511–524.

Buchert, M., Schneider, S., Meskenaite, V., Adams, M.T., Canaani, E., Baechli, T., Moelling, K., and Hovens, C.M. (1999). The junction-associated protein AF-6 interacts and clusters with specific Eph receptor tyrosine kinases at specialized sites of cell–cell contact in the brain. *J. Cell Biol.* **144**, 361–371.

Carpenter, E.M., Goddard, J.M., Davis, A.P., Nguyen, T.P., and Capocchi, M.R. (1997). Targeted disruption of *Hoxd-10* affects mouse hindlimb development. *Development* **124**, 4505–4514.

Cheng, H.J., Nakamoto, M., Bergemann, A.D., and Flanagan, J.G. (1995). Complementary gradients in expression and binding of ELF-1 and Mek4 in development of the topographic retinotectal projection map. *Cell* **82**, 371–381.

Ciossek, T., Monschau, B., Kremoser, C., Loschinger, J., Lang, S., Muller, B.K., Bonhoeffer, F., and Drescher, U. (1998). Eph receptor–ligand interactions are necessary for guidance of retinal ganglion cell axons in vitro. *Eur. J. Neurosci.* **10**, 1574–1580.

Covault, J., and Sanes, J.R. (1985). Neural cell adhesion molecule (N-CAM) accumulates in denervated and paralyzed skeletal muscles. *Proc. Natl. Acad. Sci. USA* **82**, 4544–4548.

DeSantis, M., Berger, P.K., Laskowski, M.B., and Norton, A.S. (1992). Regeneration by skeletomotor axons in neonatal rats is topographically selective at an early stage of reinnervation. *Exp. Neurol.* **116**, 229–239.

Donoghue, M.J., Merlie, J.P., Rosenthal, N., and Sanes, J.R. (1991a). Rostrocaudal gradient of transgene expression in adult skeletal muscle. *Proc. Natl. Acad. Sci. USA* **88**, 5847–5851.

Donoghue, M.J., Alvarez, J.D., Merlie, J.P., and Sanes, J.R. (1991b). Fiber type- and position-dependent expression of a myosin light chain–CAT transgene detected with a novel histochemical stain for CAT. *J. Cell Biol.* **115**, 423–434.

Donoghue, M.J., Lewis, R.M., Merlie, J.P., and Sanes, J.R. (1996). The Eph kinase ligand AL-1 is expressed by rostral muscles and inhibits outgrowth from caudal neurons. *Mol. Cell. Neurosci.* **8**, 185–198.

Dottori, M., Hartley, L., Galea, M., Paxinos, G., Polizzotto, M., Kilpatrick, T., Bartlett, P.F., Murphy, M., Kontgen, F., and Boyd, A.W. (1998). EphA4 (Sek1) receptor tyrosine kinase is required for the development of the corticospinal tract. *Proc. Natl. Acad. Sci. USA* **95**, 13248–13253.

Drescher, U., Kremoser, C., Handwerker, C., Loschinger, J., Noda, M., and Bonhoeffer, F. (1995). In vitro guidance of retinal ganglion cell axons by RAGS, a 25 kDa tectal protein related to ligands for Eph receptor tyrosine kinases. *Cell* **82**, 359–370.

Durbin, L., Brennan, C., Shiomi, K., Cooke, J., Barrios, A., Shanmugalingam, S., Guthrie, B., Lindberg, R., and Holder, N. (1998). Eph signaling is required for segmentation and differentiation of the somites. *Genes Dev.* **12**, 3096–3109.

Feldheim, D.A., Vanderhaeghen, P., Hansen, M.J., Frisen, J., Lu,

- Q., Barbacid, M., and Flanagan, J.G. (1998). Topographic guidance labels in a sensory projection to the forebrain. *Neuron* 21, 1303–1313.
- Flanagan, J.G., and Vanderhaeghen, P. (1998). The ephrins and Eph receptors in neural development. *Annu. Rev. Neurosci.* 21, 309–345.
- Freeman, R.S., Estus, S., and Johnson, E.M., Jr. (1994). Analysis of cell cycle-related gene expression in postmitotic neurons: selective induction of Cyclin D1 during programmed cell death. *Neuron* 12, 343–355.
- Frisen, J., Yates, P.A., McLaughlin, T., Friedman, G.C., O'Leary, D.D., and Barbacid, M. (1998). Ephrin-A5 (AL-1/RAGS) is essential for proper retinal axon guidance and topographic mapping in the mammalian visual system. *Neuron* 20, 235–243.
- Gale, N.W., Holland, S.J., Valenzuela, D.M., Flenniken, A., Pan, L., Ryan, T.E., Henkemeyer, M., Strebhardt, K., Hirai, H., Wilkinson, D.G., et al. (1996). Eph receptors and ligands comprise two major specificity subclasses and are reciprocally compartmentalized during embryogenesis. *Neuron* 17, 9–19.
- Gautam, M., Noakes, P.G., Moscoso, L., Rupp, F., Scheller, R.H., Merlie, J.P., and Sanes, J.R. (1996). Defective neuromuscular synaptogenesis in agrin-deficient mutant mice. *Cell* 85, 525–535.
- Hahn, C.G., and Covault, J. (1992). Neural regulation of N-cadherin gene expression in developing and adult skeletal muscle. *J. Neurosci.* 12, 4677–4687.
- Hardman, V.J., and Brown, M.C. (1987). Accuracy of reinnervation of rat internal intercostal muscles by their own segmental nerves. *J. Neurosci.* 7, 1031–1036.
- Holder, N., and Klein, R. (1999). Eph receptors and ephrins: effectors of morphogenesis. *Development* 126, 2033–2044.
- Hornberger, M.R., Dutting, D., Ciossek, T., Yamada, T., Handwerker, C., Lang, S., Weth, F., Huf, J., Wessel, R., Logan, C., et al. (1999). Modulation of EphA receptor function by coexpressed ephrinA ligands on retinal ganglion cell axons. *Neuron* 22, 731–742.
- Huynh-Do, U., Stein, E., Lane, A.A., Liu, H., Cerretti, D.P., and Daniel, T.O. (1999). Surface densities of ephrin-B1 determine EphB1-coupled activation of cell attachment through $\alpha v \beta 3$ and $\alpha 5 \beta 1$ integrins. *EMBO J.* 18, 2165–2173.
- Kilpatrick, T.J., Brown, A., Lai, C., Gassmann, M., Goulding, M., and Lemke, G. (1996). Expression of the Tyro4/Mek4/Cek4 gene specifically marks a subset of embryonic motor neurons and their muscle targets. *Mol. Cell. Neurosci.* 7, 62–74.
- Krull, C.E., Lansford, R., Gale, N.W., Collazo, A., Marcelle, C., Yancopoulos, G.D., Fraser, S.E., and Bronner-Fraser, M. (1997). Interactions of Eph-related receptors and ligands confer rostrocaudal pattern to trunk neural crest migration. *Curr. Biol.* 7, 571–580.
- Laskowski, M.B., and High, J.A. (1989). Expression of nerve-muscle topography during development. *J. Neurosci.* 9, 175–182.
- Laskowski, M.B., and Owens, J.L. (1994). Embryonic expression of motoneuron topography in the rat diaphragm muscle. *Dev. Biol.* 166, 502–508.
- Laskowski, M.B., and Sanes, J.R. (1987). Topographic mapping of motor pools onto skeletal muscles. *J. Neurosci.* 7, 252–260.
- Laskowski, M.B., and Sanes, J.R. (1988). Topographically selective reinnervation of adult mammalian skeletal muscles. *J. Neurosci.* 8, 3094–3099.
- Laskowski, M.B., Colman, H., Nelson, C., and Lichtman, J.W. (1998). Synaptic competition during the reformation of a neuromuscular map. *J. Neurosci.* 18, 7328–7335.
- Monschau, B., Kremoser, C., Ohta, K., Tanaka, H., Kaneko, T., Yamada, T., Handwerker, C., Hornberger, M.R., Loschinger, J., Pasquale, E.B., et al. (1997). Shared and distinct functions of RAGS and ELF-1 in guiding retinal axons. *EMBO J.* 16, 1258–1267.
- Nakamoto, M., Cheng, H.J., Friedman, G.C., McLaughlin, T., Hansen, M.J., Yoon, C.H., O'Leary, D.D., and Flanagan, J.G. (1996). Topographically specific effects of ELF-1 on retinal axon guidance in vitro and retinal axon mapping in vivo. *Cell* 86, 755–766.
- Ohta, K., Nakamura, M., Hirokawa, K., Tanaka, S., Iwama, A., Suda, T., Ando, M., and Tanaka, H. (1996). The receptor tyrosine kinase, Cdk8, is transiently expressed on subtypes of motoneurons in the spinal cord during development. *Mech. Dev.* 54, 59–69.
- Ohta, K., Iwamasa, H., Drescher, U., Terasaki, H., and Tanaka, H. (1997). The inhibitory effect on neurite outgrowth of motoneurons exerted by the ligands ELF-1 and RAGS. *Mech. Dev.* 64, 127–135.
- O'Leary, D.M., and Wilkinson, D.G. (1999). Eph receptors and ephrins in neural development. *Curr. Opin. Neurobiol.* 9, 65–73.
- Olivieri, G., and Miescher, G.C. (1999). Immunohistochemical localization of EphA5 in the adult human central nervous system. *J. Histochem. Cytochem.* 47, 855–861.
- Park, S., Frisen, J., and Barbacid, M. (1997). Aberrant axonal projections in mice lacking EphA8 (Eek) tyrosine protein kinase receptors. *EMBO J.* 16, 3106–3114.
- Rao, M.V., Donoghue, M.J., Merlie, J.P., and Sanes, J.R. (1996). Distinct regulatory elements control muscle-specific, fiber type-selective, and axially-graded expression of a myosin light chain gene in transgenic mice. *Mol. Cell. Biol.* 16, 3909–3922.
- Rosenthal, N., Kornhauser, J.M., Donoghue, M., Rosen, K.M., and Merlie, J.P. (1989). Myosin light chain enhancer activates muscle-specific, developmentally regulated gene expression in transgenic mice. *Proc. Natl. Acad. Sci. USA* 86, 7780–7784.
- Sanes, J.R. (1993). Topographic maps and molecular gradients. *Curr. Opin. Neurobiol.* 3, 67–74.
- Sanes, J.R., and Lichtman, J.W. (1999). Development of the vertebrate neuromuscular junction. *Annu. Rev. Neurosci.* 22, 389–442.
- Studer, M., Gavalas, A., Marshall, H., Ariza-McNaughton, L., Rijli, F.M., Chambon, P., and Krumlauf, R. (1998). Genetic interactions between Hoxa1 and Hoxb1 reveal new roles in regulation of early hindbrain patterning. *Development* 125, 1025–1036.
- Swett, J.S., Eldred, E., and Buchwald, J.S. (1970). Somatotopic cord-to-muscle relations in efferent innervation of cat gastrocnemius. *Am. J. Physiol.* 219, 762–766.
- Tiret, L., Le Mouellic, H., Maury, M., and Brulet, P. (1998). Increased apoptosis of motoneurons and altered somatotopic maps in the brachial spinal cord of Hoxc-8-deficient mice. *Development* 125, 279–291.
- Torres, R., Firestein, B.L., Dong, H., Staudinger, J., Olson, E.N., Hagan, R.L., Bredt, D.S., Gale, N.W., and Yancopoulos, G.D. (1998). PDZ proteins bind, cluster, and synaptically colocalize with Eph receptors and their ephrin ligands. *Neuron* 21, 1453–1463.
- Walter, J., Kern-Veits, B., Huf, J., Stolze, B., and Bonhoeffer, F. (1987a). Recognition of position-specific properties of tectal cell membranes by retinal axons in vitro. *Development* 101, 685–696.
- Walter, J., Henke-Fahle, S., and Bonhoeffer, F. (1987b). Avoidance of posterior tectal membranes by temporal retinal axons. *Development* 101, 909–913.
- Wang, H.U., and Anderson, D.J. (1997). Eph family transmembrane ligands can mediate repulsive guidance of trunk neural crest migration and motor axon outgrowth. *Neuron* 18, 383–396.
- Wang, H., Chadaram, S.R., Norton, A.S., Lewis, R., Boyum, J., Trumble, W., Sanes, J.R., and Laskowski, M.B. (1999). Positionally selective growth of embryonic spinal cord neurites on muscle membranes. *J. Neurosci.* 19, 4984–4993.
- Wigston, D.J., and Sanes, J.R. (1982). Selective reinnervation of adult mammalian muscle by axons from different segmental levels. *Nature* 299, 464–467.
- Wigston, D.J., and Sanes, J.R. (1985). Selective reinnervation of rat intercostal muscles transplanted from different segmental levels to a common site. *J. Neurosci.* 5, 1208–1221.
- Zhou, R. (1998). The Eph family receptors and ligands. *Pharmacol. Ther.* 77, 151–181.